Available online at www.sciencedirect.com

ScienceDirect

journal homepage: www.JournalofSurgicalResearch.com

Nondestructive Evaluation of Mechanical and Histological Properties of the Human Aorta With Near-Infrared Spectroscopy

Jaakko K. Sarin, PhD,[a,b,c,*] *Miika Kiema, MSc,*[d] *Emma-Sofia Luoto, BM,*[d] *Annastiina Husso, MD, PhD,*[e] *Marja Hedman, MD, PhD,*[e,f,g] *Johanna P. Laakkonen, PhD,*[d] *and Jari Torniainen, PhD*[c,h]

[a] *Department of Medical Physics, Medical Imaging Center, Tampere University Hospital, Tampere, Finland*
[b] *Department of Radiology, Tampere University Hospital, Tampere, Finland*
[c] *Department of Technical Physics, University of Eastern Finland, Kuopio, Finland*
[d] *A.I. Virtanen Institute for Molecular Sciences, University of Eastern Finland, Kuopio, Finland*
[e] *Department of Cardiothoracic Surgery, Kuopio University Hospital, Kuopio, Finland*
[f] *Department of Clinical Radiology, Kuopio University Hospital, Kuopio, Finland*
[g] *Institute of Clinical Medicine, University of Eastern Finland, Kuopio, Finland*
[h] *School of Information Technology & Electrical Engineering, The University of Queensland, Brisbane, Australia*

ARTICLE INFO

Article history:
Received 9 June 2022
Received in revised form
19 December 2022
Accepted 28 January 2023
Available online xxx

Keywords:
Aortic aneurysm
Biomechanics
Histology
Multivariate modeling
Spectroscopy

ABSTRACT

Introduction: Ascending aortic dilatation is a well-known risk factor for aortic rupture. Indications for aortic replacement in its dilatation concomitant to other open-heart surgery exist; however, cut-off values based solely on aortic diameter may fail to identify patients with weakened aortic tissue. We introduce near-infrared spectroscopy (NIRS) as a diagnostic tool to nondestructively evaluate the structural and compositional properties of the human ascending aorta during open-heart surgeries. During open-heart surgery, NIRS could provide information regarding tissue viability *in situ* and thus contribute to the decision of optimal surgical repair.

Materials and methods: Samples were collected from patients with ascending aortic aneurysm ($n = 23$) undergoing elective aortic reconstruction surgery and from healthy subjects ($n = 4$). The samples were subjected to spectroscopic measurements, biomechanical testing, and histological analysis. The relationship between the near-infrared spectra and biomechanical and histological properties was investigated by adapting partial least squares regression.

Results: Moderate prediction performance was achieved with biomechanical properties ($r = 0.681$, normalized root-mean-square error of cross-validation = 17.9%) and histological properties ($r = 0.602$, normalized root-mean-square error of cross-validation = 22.2%). Especially the performance with parameters describing the aorta's ultimate strength, for example, failure strain ($r = 0.658$), and elasticity (phase difference, $r = 0.875$) were promising and could, therefore, provide quantitative information on the rupture sensitivity of the aorta. For the estimation of histological properties, the results with α-smooth muscle actin ($r = 0.581$), elastin density ($r = 0.973$), mucoid extracellular matrix accumulation($r = 0.708$), and media thickness ($r = 0.866$) were promising.

* *Corresponding author*. Department of Medical Physics, Medical Imaging Center, Tampere University Hospital, Tampere, Finland.
E-mail address: jaakko.sarin@pirha.fi (J.K. Sarin).

https://doi.org/10.1016/j.jss.2023.01.016

Conclusions: NIRS could be a potential technique for *in situ* evaluation of biomechanical and histological properties of human aorta and therefore useful in patient-specific treatment planning.

Introduction

Cardiovascular disorders are the number one cause of global mortality.[1] Ascending aortic aneurysm (AA), also referred to as the silent killer, is asymptomatic in up to 95% of the cases.[2] The increased diameter of the AA is a well-known risk factor for aortic rupture[3]; nevertheless, there is a growing interest in the impact of aortic wall thickness and structure predisposing to rupture. AA is often incidentally detected and due to its high mortality in case of rupture, AAs are closely monitored[4] and eventually, prophylactic aortic reconstructive surgery is performed.

Current noninvasive imaging techniques of AA estimation are computed tomography (CT) and magnetic resonance imaging (MRI).[3] Recently, AA has been investigated with novel MRI sequences that have enabled the evaluation of blood flow velocity and direction (4D flow sequence),[5] and thereby the estimation of forces experienced by the aortic wall. However, variations in tissue properties between patients (e.g., aortic wall thickness and stiffness)[6] make patient-specific rupture estimation challenging.

Currently, the tissue properties may only be destructively determined from the extracted tissue samples by utilizing *in vitro* techniques, such as biomechanical testing and histology, making them unsuitable for clinical patients. A potential technique for *in vivo* evaluation of tissue properties is near-infrared spectroscopy (NIRS) – previously applied in orthopedic surgeries[7,8] and dermatological applications.[9] The technique utilizes nonionizing light and can enable subsecond evaluation of tissue. However, the technique requires direct contact between the measurement device and the target tissue, thus making the technique only applicable during open-heart surgeries.

Current guidelines[10,11] recommend isolated ascending aortic replacement when aortic diameter reaches 55 mm and replacement of ascending aorta concomitant to aortic valve surgery when diameter reaches 45 mm. Several risk factors (e.g., bicuspid aortic valve (BAV) and genetic connective tissue disorders) predispose earlier replacement; however, patients undergoing other open-heart surgery (e.g., mitral valve repair or coronary artery bypass) are not included in the current guidelines. In addition, patients close to the diameter thresholds are often encountered and thus patient-specific decision-making is crucial. The possibility to evaluate the integrity of the ascending aorta in the operating room (OR) would be especially beneficial for patients with AA (diameter over 40 mm) but not meeting the current criteria for the aortic replacement at the time of their other open-heart surgery. The *in vivo* evaluation could also enable to map the extent of the deterioration, thereby limiting the amount of tissue to be replaced (e.g., only ascending aorta or the whole aortic arch).

We hypothesize that NIRS could enable the characterization of the biomechanical and histological properties of the aorta. Application of the technique during open-heart surgery could substantially contribute to the decision on the optimal repair approach. To test the hypothesis, samples were collected from patients undergoing elective ascending aortic surgery and the extracted samples were subjected to vigorous laboratory measurements to investigate their relationship with near-infrared (NIR) spectra.

Materials and Methods

Ascending AA samples were collected from patients with bicuspid (BAV) and tricuspid aortic valves (TAV) ($n = 23$ [$n_{BAV} = 8$, $n_{TAV} = 15$], age $= 64.0 \pm 7.7$) during an elective aortic reconstruction surgery at Kuopio University Hospital, Finland (Table 1).[12] Patients with mechanical aortic valve or genetic disorders were excluded. In addition, control samples were collected from organ donors ($n = 4$, age $= 59.3 \pm 9.7$) with TAV, no history of major cardiovascular diseases, and normal aortic dimensions (based on CT after admission).[12] None of the patients or controls had a ruptured or dissected AA. During the surgery, a section of AA was resected and divided into proximal (closer to heart) and distal (farther out from heart) arterial rings which were subjected to spectral and biomechanical measurements and histology, respectively. The proximal part was immersed in saline and refrigerated, followed by post-haste subjection to spectral and biomechanical measurements. The distal part was fixed in 4% paraformaldehyde, followed by histological preparation and analysis. All specimens were treated identically during reference analysis. The study was approved by the research ethics committee of the Northern Savo Hospital District (permission number 200/2017), had an organization permit of Kuopio University Hospital for processing personal data, and followed the declaration of Helsinki. Written informed consent was obtained from every patient.

Near-infrared spectroscopy

From the proximal section, circumferential dumbbell-shaped specimens (length ~ 10 mm) were extracted with a custom punch tool from both the inner and outer curves (Fig. 1A). The specimen type was chosen based on the hardware available and the extensive previous research to validate our measurement parameters.[13] The specimens were subjected to spectroscopy measurements from five equidistant locations (~2 mm apart). For each location, three spectra (each average of 100 acquisitions) were recorded by aligning the optical probe (Fig. 1B) in contact with the specimen adventitia. The hardware consisted of two spectrometers (AvaSpec-ULS2048L,

Table 1 – Patient demographics.

	Patients	BAV	TAV	Controls (TAV)
n	23	8	15	4
Age	64.0 ± 7.7	59.0 ± 8.1	66.6 ± 6.1	59.3 ± 8.4
Gender (male/female)	19/4	7/1	12/3	3/1
Body mass index	28.5 ± 3.1	30.1 ± 3.1	27.7 ± 2.7	NA
Hypertension (*n*)	15 (65.2%)	5 (62.5%)	10 (66.7%)	2 (50.0%)
Dyslipidemia (*n*)	13 (56.5%)	5 (62.5%)	8 (53.3%)	1 (25.0%)
Diabetes (*n*)	1 (4.3%)	0 (0.0%)	1 (6.7%)	2 (50.0%)
Coronary artery disease (*n*)	2 (8.7%)	1 (12.5%)	1 (6.7%)	0 (0.0%)
Medication, statins (*n*)	12 (52.2%)	3 (37.5%)	9 (60.0%)	0 (0.0%)
The largest diameter of AA (mm)	52.9 ± 4.0	49.8 ± 3.5	54.6 ± 3.1	36.1 ± 3.9
Aortic regurgitation (*n*)	14 (60.9%)	5 (62.5%)	9 (60.0%)	0 (0.0%)
Aortic stenosis (*n*)	2 (8.7%)	2 (25.0%)	0 (0.0%)	0 (0.0%)

$\lambda = 0.35–1.1$ μm, $\Delta\lambda = 0.6$ nm and AvaSpec-NIR256-2.5-HSC, $\lambda = 1.0–2.5$ μm, $\Delta\lambda = 6.4$ nm, Avantes BV, Apeldoorn, Netherlands), a light source (AvaLight-HAL-(S)-Mini, $\lambda = 0.36–2.5$ μm, Avantes BV) and an optical probe. The robust optical probe is sterilizable and has been previously applied in *ex vivo* and *in vivo* arthroscopies.[8,14]

Reference analysis

For biomechanical measurements (Fig. 2), a dumbbell-shaped specimen was attached to testing clamps of the commercial mechanical tester (Mach-1 v500 css, Biomomentum Inc, Laval, Canada) that was used with two load cells (17N, MA239, and 250N, MA297, Biomomentum Inc). The specimen's wall thickness and width were determined with a caliper. The specimen was preloaded (stress = 10 kPa), preconditioned (10 × 2% strain), and recovered before protocol execution. The protocol consisted of sequential stress relaxation, sinusoidal, and quasistatic stages that were used to calculate equilibrium modulus, dynamic modulus and phase difference, and quasistatic material properties (e.g., failure strain, linear modulus, and fitting parameters for the toe region), respectively.

Histological analyses were performed on the distal part of the aorta with segments taken from the inner and outer curves. Verhoeff–Van Gieson elastin staining (HT25 A, Merck, Darmstadt, Germany) was performed according to the manufacturer's protocol from which medial degeneration was scored on a scale of 0–3 according to Halushka *et al.*[15] by assessing the following parameters: mucoid extracellular matrix accumulation, elastic fiber fragmentation and/or loss, smooth muscle cell nuclei loss, and laminar medial collapse. In addition, media thickness and the amount of elastin per area (elastin density) were analyzed. Collagen content was not determined as previous studies have highlighted elastin as a more descriptive parameter for aneurysmal tissue.[16] Primary antibodies used for immunohistochemistry were the following: smooth muscle cell marker alpha-smooth muscle actin (α-SMA, M0851, Agilent Technologies, Santa Clara, CA), T-cell marker CD3 (M7254, Agilent Technologies), and macrophage marker CD68 (M0814, Agilent Technologies). Biotinylated horse antimouse IgG (BA-2000, Vector Laboratories, Burlingame, CA) was used as a secondary antibody. Tissue sections were imaged with a Nanozoomer-XR Digital slide scanner (Hamamatsu, Hamamatsu City, Japan) in Biobank of Eastern Finland (Kuopio, Finland). Image analysis was performed with Aperio ImageScope software (Leica Biosystems, Wetzlar, Germany).

Spectral preprocessing

Spectral preprocessing is essential when relating the spectrum with tissue properties due to, for example, noise and

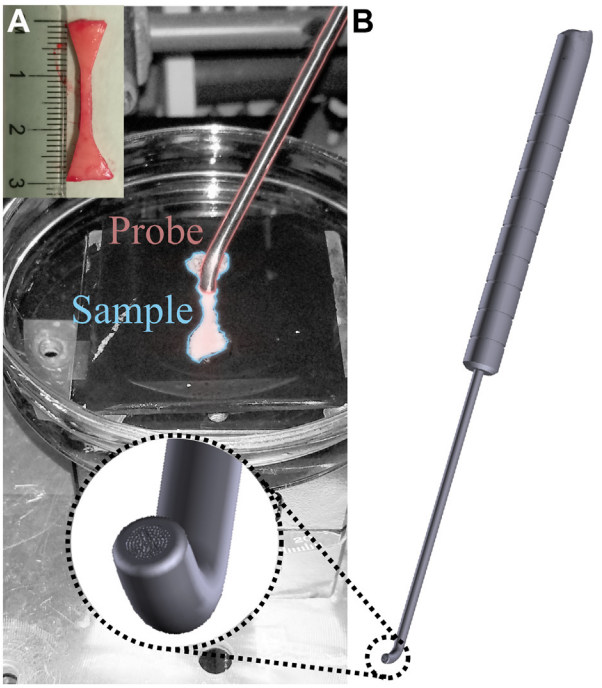

Fig. 1 – Near-infrared spectroscopy (NIRS) measurement system. The dumbbell-shaped specimens were placed on a sample holder of nonrefracting material and submerged to keep the samples hydrated (A). A sterilizable and clinically applicable custom probe was used to record spectra (B).

scatter.[17] In this study, spectral resolution from the 1st spectrometer ($\Delta\lambda = 0.6$ nm) was downsampled to the same resolution as the 2nd spectrometer ($\Delta\lambda = 6.4$ nm) and concatenated to ease preprocessing. An open-source preprocessing module nippy[18] was used in Python 3.7 to explore the effect of preprocessing on model performance. Smoothing, scatter correction techniques, and trimming were included as operators. A 3rd-degree Savitzky–Golay filter with 0th (i.e., smoothing), 1st, and 2nd derivatives with different filter windows (7+8i, i = 1–5) were evaluated. For normalization, standard normal variate (SNV) and localized SNV (LSNV, windows = 2+4i, i = 1–4) were tested. The analysis was tested with the following spectral regions: 0.40–2.50 μm, 0.40–1.90 μm, 0.40–1.375 μm and 1.525–1.90 μm, and 0.70–1.375 μm and 1.525–1.90 μm.

Outliers and multivariate modeling

Prior to modeling, univariate (i.e., biomechanical and histological properties) and multivariate (i.e., spectra) outliers were investigated. For normal and non-normal data distributions, univariate values with the offset of three or higher standard deviations or median absolute deviations, respectively, were further investigated. Two outlier spectra were observed (hardware-related errors). In addition, the extended isolation forest (EIF, trees = 500, sample = 100)[19] was used to investigate the presence of outliers in the preprocessed spectra. EIF was used for each preprocessing normalization window. The optimal EIF threshold for outliers was investigated.

To avoid overfitting and bias in the modeling, 5-fold cross-validation with stratified groups (i.e., patient's measurements together in a group) were used. In the modeling, the median performance of partial least squares regression (PLSR) over 10 iterations (unique 5-fold cross-validation sets) was determined and the optimal preprocessing was chosen based on the minimum root-mean-square error of cross-validation (RMSECV). The models were trained with the average spectrum calculated from the nonoutlier spectra.

Statistical analysis

Statistical testing and model building was performed in Matlab (R2020a, Mathworks, Natick, MA). Mann–Whitney U-test was used to estimate statistical significance between patient and control samples. Values are presented as median (interquartile range, IQR).

Data of the current study is available from the author on a reasonable request.

Results

Based on the patient demographics, AA was substantially more common among men (Table 1). Due to the uneven gender distribution with a relatively low number of patients, statistical analyses related to patient demographics were not performed.

As a result of the two sample reference processing pipelines (histology and biomechanics) and two different load cells in biomechanics, the number of measurements varied depending on the reference variable (Table 2). Although some reference values exceeded the threshold of 3 standard deviations or median absolute deviation, no value was excluded after ensuring the data validity. For the exclusion of spectral outliers (Fig. 3A-B), the EIF threshold of 0.7 was optimal based on the overall validation performance, thereby resulting in 12 (14) outliers (median (IQR)).

Overall, NIR spectra were superior in predicting AA's biomechanical properties ($r = 0.660$, normalized RMSECV = 17.8%) compared to the histological properties (Table 2, $r = 0.600$, normalized RMSECV = 22.2%). Group comparison (patient and control) revealed that on average the relative validation error (group-specific RMSECV *versus* overall RMSECV) was slightly higher with patients (+3%) compared to controls (−9%). Most promisingly, the ultimate and dynamic properties from biomechanical testing had moderate performance and, therefore, provide quantitative information on the rupture sensitivity (Fig. 4A and B). For estimation of histological properties, especially the results on the α-SMA, elastin density, mucoid extracellular matrix accumulation, and media thickness are promising (Fig. 4C and D).

With measured reference values, statistical significance was observed between patient and control groups with α-SMA in the inner curve ($P = 0.023$) and with CD68 in the outer curve ($P = 0.036$). Related to these references, statistical differences were also observed with the predicted values of the models

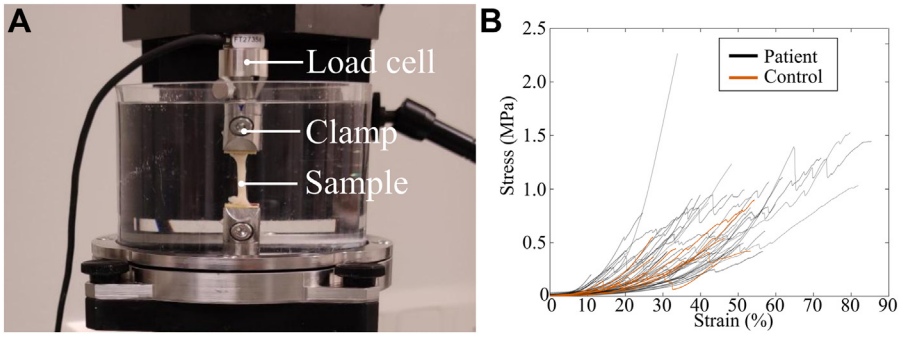

Fig. 2 – Uniaxial biomechanical measurement system. The specimens were subjected to extensive reference analysis (i.e., biomechanics (A) and histology). The strain-stress curves of the ultimate biomechanical uniaxial test for each specimen are presented (B).

Table 2 – Performance metrics of the PLSR models.

Reference parameter	N	Median (IQR)	n	R	RMSE	RMSECV
Biomechanics						
Equilibrium modulus (MPa)	40	0.224 (0.215)	2 (1)	0.489 (0.073)	0.205 (0.009)	0.218 (0.013)
Dynamic modulus (MPa)	40	0.377 (0.545)	1 (0)	0.508 (0.003)	0.533 (0.002)	0.533 (0.021)
Phase difference (°)	40	3.950 (0.991)	3 (0)	0.875 (0.003)	0.344 (0.006)	0.463 (0.048)
Toe fit - A	52	4.040 (4.947)	2 (0)	0.565 (0.007)	3.315 (0.016)	3.525 (0.164)
Toe fit - B	52	−0.248 (0.271)	5 (4)	0.744 (0.182)	0.146 (0.046)	0.200 (0.009)
Toe fit - C	52	0.014 (0.019)	4 (0)	0.906 (0.005)	0.006 (0.000)	0.013 (0.002)
Linear modulus (MPa)	52	4.120 (2.306)	3 (0)	0.905 (0.007)	0.960 (0.012)	2.064 (0.178)
Failure energy (mJ)	52	3.011 (5.459)	2 (0)	0.604 (0.002)	2.990 (0.012)	3.257 (0.063)
Failure energy per V (J/m3)	52	34.19 (65.86)	2 (0)	0.543 (0.009)	47.45 (0.205)	50.33 (3.349)
Failure force (n)	52	2.329 (1.592)	2 (0)	0.646 (0.006)	0.996 (0.006)	1.113 (0.018)
Failure strain (%)	52	43.82 (20.22)	2 (0)	0.667 (0.003)	11.80 (0.041)	13.04 (0.263)
Failure stress (MPa)	52	0.578 (0.490)	2 (0)	0.464 (0.006)	0.343 (0.002)	0.353 (0.012)
Histology						
α-SMA	50	0.355 (0.105)	4 (2)	0.581 (0.115)	0.075 (0.007)	0.085 (0.002)
CD3	50	1.325 (0.400)	1 (0)	0.434 (0.006)	0.334 (0.002)	0.346 (0.011)
CD68	50	0.800 (0.400)	2 (1)	0.451 (0.019)	0.320 (0.004)	0.344 (0.008)
Degeneration	52	2.00 (0.50)	1 (0)	0.309 (0.004)	0.509 (0.002)	0.531 (0.014)
Elastin density	52	0.179 (0.087)	7 (3)	0.973 (0.023)	0.015 (0.006)	0.065 (0.009)
MEMA	50	1.50 (1.00)	4 (1)	0.708 (0.054)	0.318 (0.025)	0.434 (0.008)
Media thickness (mm)	52	1.67 (0.30)	7 (2)	0.866 (0.044)	0.144 (0.023)	0.239 (0.022)
SMC nuclei loss	50	2.00 (1.00)	1 (0)	0.369 (0.008)	0.603 (0.004)	0.658 (0.026)
SMC loss	50	1.667 (0.667)	1 (0)	0.439 (0.015)	0.335 (0.003)	0.346 (0.021)

The number of measurements and values (median with interquartile range ([IQR, in brackets]) for the reference properties is presented. For the PLSR models, statistics (median and IQR (in brackets) of 10 iterations) for the number of components (*n*), Pearson correlation (*r*), root-mean-square-error (RMSE) and RMSE of cross-validation (RMSECV) are presented.

($P = 0.023$ and $P = 0.029$, respectively), thus further validating model performances.

The assessment of optimal preprocessing pipelines revealed the importance of spectral normalization (86% of models) with 92% of these using LSNV. In addition, the relative performance (RMSECV/RMSE) was substantially better for the models that did not utilize the spectral region 1.9–2.5 μm. Overall, the combination of spectral regions 0.7–1.375 μm and 1.525–1.9 μm had the best performance.

Discussion

In this study, we hypothesized that NIRS could enable the evaluation of biomechanical competence and histological properties of the aorta. The spectral measurements were performed with the sterilizable probe directly applicable in open-heart surgeries. The results indicated that NIRS is capable to estimate the biomechanical competence and to some extent the histological properties of ascending aorta. Therefore, NIRS could be valuable especially for the patients in the gray zone according to current guidelines regarding replacement of the AA, particularly simultaneous to other open-heart surgery.[10,11]

Current clinical imaging techniques are not directly adaptable to evaluate the biomechanical[20] or histological properties of the aorta. Liu *et al*. demonstrated on two patients that the combination of clinical CT images and modeling may be suited for the estimation of AA wall properties.[21] Modeling always, however, suffers from parameter assumptions and compared to the resolution of CT scanners, reliable estimation of aortic wall thickness may be challenging. In our study, the wall thickness could be reliably assessed with 0.2 mm precision. Intraoperative speckle transesophageal

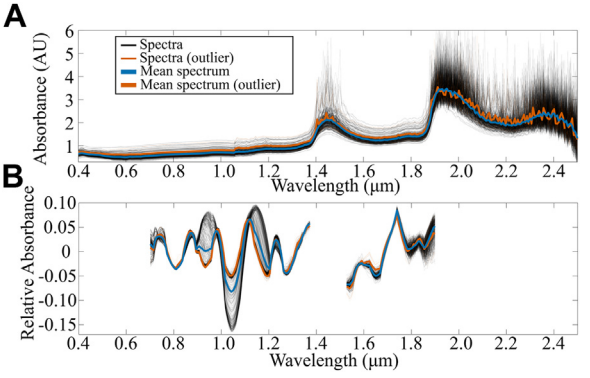

Fig. 3 – The near-infrared (NIR) spectra of the specimens. The raw (A) and preprocessed (B, optimal for failure strain) spectra are presented with their means and the outliers (determined with extended isolation forest).

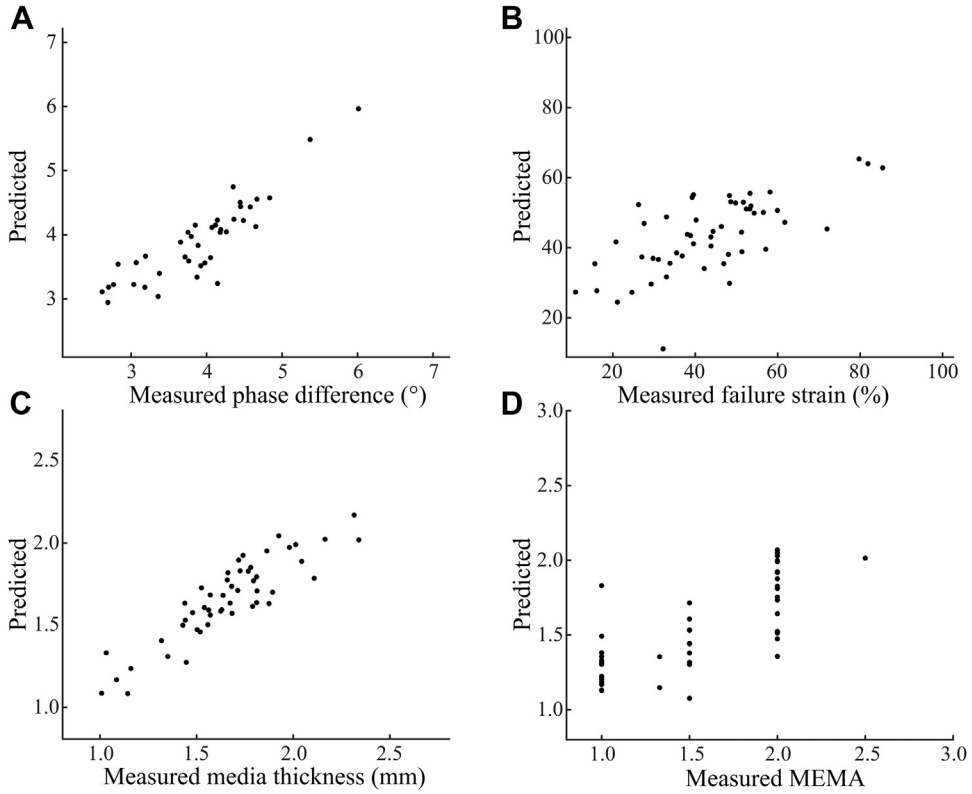

Fig. 4 – Prediction performance of representative PLSR models. Scatter plots between the measured and median predictions of the cross-validated models for phase difference (A), failure strain (B), media thickness (C), and mucoid extracellular matrix accumulation (MEMA, (D) are presented.

echocardiography was introduced by Alreshidan *et al.*, but no significant correlation was observed between the *in vivo* and *ex vivo* stiffness.[22] Another method is based on magnetic resonance elastography, which may enable the evaluation of aorta's mechanical properties.[20] The imaging is known to be challenging and requires long imaging time[20]; however, a correlation between magnetic resonance elastograph-derived stiffness and elastin density has been reported.[23] Here, we demonstrated a high correlation between NIR spectra and elastin density.

The demonstrated relationships between spectra and reference properties arise from the light interactions with the tissue.[24] The most abundant chemical bonds of the aorta are OH, CH, SH, and NH that associate with specific spectral regions.[24] The effect of water (OH bond) is the most pronounced in the spectral response of the aorta (Fig. 3A, 1.45 and 1.95 μm). Spectral changes (Fig. 3B) were especially observed in the spectral regions of 0.92, 1.04, and 1.15 μm which correspond to the third overtones of CH/ROH, the third overtone of RNH2, and the second overtone of CH3, respectively. For example in elastin and collagen, these bonds are common, thereby arguably contributing to the high prediction accuracy.

The spectral preprocessing had a substantial effect on model performance, as also previously described.[17,18] The most reliable performance was achieved by excluding/trimming the spectral regions of water peaks where a relatively poor signal-to-noise ratio was observed (Fig. 3B). Another key aspect is the presence of outliers (especially for *in vivo* measurements[8]) and their reliable exclusion. Here, a recently introduced EIF algorithm was used with a nontraditional threshold of 0.7. Previously, the threshold of one has been used, but this threshold did not exclude abnormal spectra in our study, thus highlighting the importance of spectral visualization and outlier investigation.

Although the results of the current study are promising, further validation is required in the form of additional reference information. In addition, the performance may improve by adapting nonlinear algorithms[25] or machine learning[26] approaches. The next logical step is to further validate the models and employ these in a clinical situation, for example, with patients undergoing a valve replacement with an aortic diameter of 40–49 mm. Another intriguing possibility is spectroscopic imaging,[27] which does not require direct contact with the tissue (but visualization) and enables swift imaging (one image) and thus quantification of the visualized tissue. The number of patients recruited and especially the uneven gender distribution is a limitation to this study. Although the study does not focus on aortopathy prevalence or progression, the reference information (i.e., biomechanics and histology) better describes the characteristics of male patients. Thus, further validation is required with more gender-balanced datasets.

Based on the current guidelines, *in vivo* integrity evaluation of the ascending aorta would be especially beneficial for patients with aortic diameter over 40 mm but not meeting the current criteria for the aortic replacement at the time of their other open-heart surgery. NIRS is a promising technique for *in situ* evaluation of ascending aorta biomechanical and

histological properties during the surgery and thereby could enhance patient-specific treatment. This study highlights the potential of NIRS for the estimation of the aorta's biomechanical and histological properties. For future works, acquiring additional data enables the usage of more sophisticated algorithms, thereby arguably improving prediction accuracy and, thus, enabling clinical *in vivo* estimation of aortic properties.

Author Contributions

Sarin, J.K.: Study design, data acquisition, data analysis, writing - original draft. Kiema, M.: Data acquisition, writing–review & editing. Luoto, E–S.: Data acquisition, writing–review & editing. Husso, A.; Conducting the clinical study, data interpretation, writing–review & editing. Hedman, M.: Conducting the clinical study, data interpretation, writing–review & editing. Laakkonen, J.P.: Data interpretation, writing–review & editing. Torniainen, J.: Study design, data acquisition, writing - review & editing. All authors approved of the final submitted manuscript.

Acknowledgments

The authors wish to thank the personnel of Kuopio University Hospital, particularly Petri Toroi and Pekka Jaakkola. This work was supported by the Academy of Finland (JPL 321535 and 328835), Finnish Foundation of Cardiovascular Diseases (JPL) and Oiva Vaittinen will donation (18405). There are no relationships with the industry.

Disclosure

Hedman, M. wishes to disclose professional lectures for Siemens Healthineers and GE corporations. In addition, she is a board member of the Finnish Cardiac Society. The other authors report no proprietary or commercial interest in any product mentioned or concept discussed in this article.

Funding

None.

REFERENCES

1. Roth GA, Mensah GA, Johnson CO, et al. Global burden of cardiovascular diseases and risk factors, 1990–2019: update from the GBD 2019 study. *J Am Coll Cardiol*. 2020;76:2982–3021.
2. Elefteriades JA, Sang A, Kuzmik G, Hornick M. Guilt by association: paradigm for detecting a silent killer (thoracic aortic aneurysm). *Open Hear*. 2015;2:e000169.
3. Erbel R, Aboyans V, Boileau C, et al. 2014 ESC guidelines on the diagnosis and treatment of aortic diseases. *Eur Heart J*. 2014;35:2873–2926.
4. Benedetti N, Hope MD. Prevalence and significance of incidentally noted dilation of the ascending aorta on routine chest computed tomography in older patients. *J Comput Assist Tomogr*. 2015;39:109–111.
5. Dyverfeldt P, Bissell M, Barker AJ, et al. 4D flow cardiovascular magnetic resonance consensus statement. *J Cardiovasc Magn Reson*. 2015;17:1–19.
6. Xuan Y, Wisneski AD, Wang Z, et al. Regional biomechanical and failure properties of healthy human ascending aorta and root. *J Mech Behav Biomed Mater*. 2021;123:104705.
7. Spahn G, Plettenberg H, Kahl E, Klinger HM, Mückley T, Hofmann GO. Near-infrared (NIR) spectroscopy. A new method for arthroscopic evaluation of low grade degenerated cartilage lesions. Results of a pilot study. *BMC Musculoskelet Disord*. 2007;8:47.
8. Sarin JK, te Moller NCR, Mohammadi A, et al. Machine learning augmented near-infrared spectroscopy: in vivo follow-up of cartilage defects. *Osteoarthr Cartil*. 2021;29:423–432.
9. McIntosh LM, Jackson M, Mantsch HH, Mansfield JR, Crowson AN, Toole JWP. Near-infrared spectroscopy for dermatological applications. *Vib Spectrosc*. 2002;28:53–58.
10. Vahanian A, Beyersdorf F, Praz F, et al. 2021 ESC/EACTS Guidelines for the management of valvular heart disease. *Eur Heart J*. 2021;43:561–632.
11. Hiratzka LF, Bakris GL, Beckman JA, et al. 2010 ACCF/AHA/AATS/ACR/ASA/SCA/SCAI/SIR/STS/SVM guidelines for the diagnosis and management of patients with thoracic aortic disease. *Circulation*. 2010;121:e266–e369.
12. Kiema M, Sarin JK, Kauhanen SP, Torniainen J, Matikka H. Wall shear stress predicts media degeneration and biomechanical changes in thoracic aorta. *Front Physiol*. 2022;13:934941.
13. Avanzini A, Battini D, Bagozzi L, Bisleri G. Biomechanical evaluation of ascending aortic aneurysms. *BioMed Res Int*. 2014;2014:820385.
14. Prakash M, Joukainen A, Torniainen J, et al. Near-infrared spectroscopy enables quantitative evaluation of human cartilage biomechanical properties during arthroscopy. *Osteoarthr Cartil*. 2019;27:1235–1243.
15. Halushka MK, Angelini A, Bartoloni G, et al. Consensus statement on surgical pathology of the aorta from the Society for Cardiovascular Pathology and the Association for European Cardiovascular Pathology: II. Noninflammatory degenerative diseases - nomenclature and diagnostic criteria. *Cardiovasc Pathol*. 2016;25:247–257.
16. Iliopoulos DC, Kritharis EP, Giagini AT, Papadodima SA, Sokolis DP. Ascending thoracic aortic aneurysms are associated with compositional remodeling and vessel stiffening but not weakening in age-matched subjects. *J Thorac Cardiovasc Surg*. 2009;137:101–109.
17. Rinnan Å, van den BF, Engelsen SB. Review of the most common pre-processing techniques for near-infrared spectra. *TrAC Trends Anal Chem*. 2009;28:1201–1222.
18. Torniainen J, Afara IO, Prakash M, Sarin JK, Stenroth L, Töyräs J. Open-source python module for automated preprocessing of near infrared spectroscopic data. *Anal Chim Acta*. 2020;1108:1–9.
19. Hariri S, Kind MC, Brunner RJ. Extended isolation forest. *IEEE Trans Knowl Data Eng*. 2018;33:1479–1489.
20. Khan S, Fakhouri F, Majeed W, Kolipaka A. Cardiovascular magnetic resonance elastography: a review. *NMR Biomed*. 2018;31:e3853.
21. Liu M, Liang L, Sulejmani F, et al. Identification of in vivo nonlinear anisotropic mechanical properties of ascending thoracic aortic aneurysm from patient-specific CT scans. *Sci Rep*. 2019;9:12983.
22. Alreshidan M, Shahmansouri N, Chung J, et al. Obtaining the biomechanical behavior of ascending aortic aneurysm via the

use of novel speckle tracking echocardiography. *J Thorac Cardiovasc Surg*. 2017;153:781–788.
23. Dong H, Dong H, Russell DS, et al. In vivo aortic magnetic resonance elastography in abdominal aortic aneurysm: a validation in an animal model. *Invest Radiol*. 2020;55:463–472.
24. Burns DA, Ciurczak EW. *Handbook of Near-Infrared Analysis*. 3rd ed. Boca Raton, FL: CRC Press; 2007.
25. Cui C, Fearn T. Comparison of partial least squares regression, least squares support vector machines, and Gaussian process regression for a near infrared calibration. *J Near Infrared Spectrosc*. 2017;25:5–14.
26. Cui C, Fearn T. Modern practical convolutional neural networks for multivariate regression: applications to NIR calibration. *Chemom Intell Lab Syst*. 2018;182:9–20.
27. Halicek M, Fabelo H, Ortega S, Callico GM, Fei B. In-vivo and ex-vivo tissue analysis through hyperspectral imaging techniques: revealing the invisible features of cancer. *Cancers*. 2019;11:1–30.